Electrical properties of poly(2,5-thienylene vinylene) films doped with iodine*

W. Eevers, M. De Wit, J. Briers and H. J. Geise†
University of Antwerp (UIA), Department of Chemistry, Universiteitsplein 1, B-2610 Wilrijk, Belgium

and R. Mertens, P. Nagels and R. Callaerts
University of Antwerp (RUCA), Middelheimlaan 1, B-2020 Antwerp, Belgium

and W. Herrebout and B. Van der Veken
University of Antwerp (RUCA), Department of Inorganic Chemistry, Groenenborgerlaan 171, B-2020 Antwerp, Belgium

Films of poly(2,5-thienylene vinylene) (PTV) were prepared via thermal elimination under vacuum of an HCl-treated methoxy precursor polymer. Optimum reaction conditions were obtained from on-line Fourier transform infra-red experiments. Doping was achieved either by immersing the PTV films in a solution of $^{129}I_2$ in pentane or by exposing them to I_2 vapour. The doping level of the samples was measured by electron probe X-ray micro-analysis; values of the iodine/sulfur atomic ratio ranged from 0.4 to 0.57. Dopant profiles were determined on sections of the doped films by scanning electron microscopy–energy dispersive spectral analysis. Electron microscopy also revealed the porous structure of the PTV films, rationalizing the ease with which the dopant penetrates. Despite the porosity, the films could be doped homogeneously and reproducibly. Mössbauer spectroscopy showed that predominantly I_5^- is present as the dopant species, which leads to one dopant ion per 10–13 monomeric units. The temperature dependence of the d.c. conductivity (measured between 90 and 300 K) is best described by variable-range hopping (VRH) in three dimensions. Using Mott's formulae the physical parameters involved in VRH, i.e. the density of states at the Fermi level, the hopping distance and hopping energy, are calculated.

(Keywords: poly(thienylene vinylene); iodine doping; electrical properties)

INTRODUCTION

Interest in poly(2,5-thienylene vinylene) (PTV) is growing, for a number of reasons. For example, it is a π-conjugated, rigid polymer with good thermal stability. Its electron-rich thiophene rings help to stabilize acceptor-doped derivatives by lowering the chemical potential of the ionized complexes to the point where they will no longer be reduced by water vapour[1]. In comparison with poly(*p*-phenylene vinylene), PTV shows higher conductivities upon doping[2]. Furthermore, the synthesis via a so-called soluble precursor method has greatly improved the processibility[3-6]. The advantage is that the methoxy precursor polymer is soluble in organic solvents and can easily be converted into the final, conjugated polymer films. Another advantage of PTV is the presence of a sulfur atom in each monomer unit, which can be used as an internal standard, e.g. in the quantitative analysis of the doped polymer by X-ray micro-analysis.

No systematic characterization of the doping of PTV has been reported yet. The objective of the present study is to clarify the chemistry and the conduction mechanism upon reaction of PTV with iodine, administered either in the vapour phase, or in pentane solution. Therefore, the quality of the PTV films used was monitored by on-line Fourier transform infra-red (*FT*i.r.) measurements during the elimination reaction of the precursor polymer to the fully conjugated material. Because of the difficulties in obtaining homogeneously doped films, bulk analyses of the doped films are not unequivocal. These problems are circumvented by examining thin layers of the doped materials by electron probe X-ray micro-analysis (EPXMA) and scanning electron microscopy (SEM). In order to obtain information about the mechanism of the charge transport in lightly and in heavily doped PTV, the temperature dependence of the d.c. conductivity is measured between 90 and 300 K. The nature of the dopant species is derived from Mössbauer spectroscopy.

EXPERIMENTAL

The methoxy precursor of PTV was synthesized as reported before[7]. Complete elimination was then achieved by first treating a chloroform solution of the precursor with concentrated hydrochloric acid, followed by casting

* Presented at 'The Polymer Conference', 20–22 July 1993, University of Cambridge, UK

† To whom correspondence should be addressed

0032-3861/94/21/4573-05

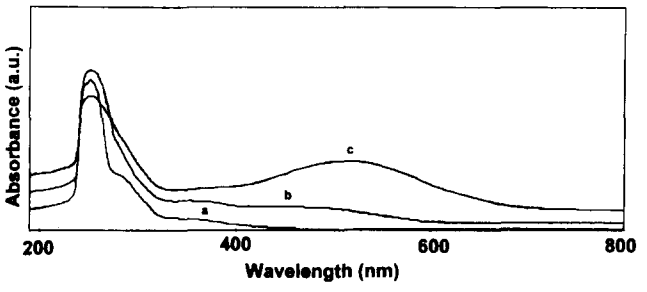

Figure 1 Evolution of the u.v./vis. spectrum of a chloroform solution of the methoxy precursor of PTV treated with concentrated hydrochloric acid: (a) untreated precursor; (b) treated precursor after 5 min at room temperature; (c) as (b), but after 30 min

of a film of about 50 μm thickness and heating the film at 120°C *in vacuo* for 3 h. The optimum elimination conditions had been obtained before from *FT*i.r. experiments in which methoxy precursor films of HCl-treated solutions were cast on potassium bromide discs mounted in the high-temperature vacuum infra-red cell of a Bruker IFS 113 v, and the spectra recorded in the temperature range 20–250°C.

In one series of experiments iodine doping was performed by exposing optimally eliminated PTV films to iodine vapour in a glass reactor immersed in a thermostated bath; the temperatures were 40°C (corresponding to an I_2 vapour pressure of 133 Pa) and 72°C (corresponding to an I_2 vapour pressure of 1333 Pa). During these processes the doping levels were monitored by continuously measuring the conductivity with the two-probe d.c. technique. In the other series of experiments doping was performed at room temperature by soaking the PTV films for various times in pentane solutions of I_2; as concentrations we used 7×10^{-2} M (saturated solution) and 4×10^{-2} M, 3.1×10^{-2} M, 1.55×10^{-2} M and 0.775×10^{-2} M.

After doping, the films were washed with pure pentane, dried under nitrogen and cut to the desired size: circular pieces of 20 mm diameter for Mössbauer experiments (see below) and 15 x 5 mm for d.c. conductivity measurements. Two gold electrodes were sputtered on each end of the specimen and the conductivity measured in the range 90–300 K.

The Mössbauer determinations required the use of the radioactive $^{129}I_2$ (half-life 1.57×10^7 year), because of the better spectroscopic properties of this isotope[8,9]. We started from an aqueous solution of $Na^{129}I$ stabilized with Na_2SO_3, and oxidized it with 6 N sulfuric acid and a 10% H_2O_2 solution. Then the $^{129}I_2$ was extracted with pentane and used for solution doping. For safety reasons, the processes were performed in specially designed, sealed vessels[10]. Doped films were mounted in a poly(methyl methacrylate) holder. As Mössbauer source $Mg_3{}^{129m}TeO_6$ (supplied by Energie Centrum Nederland, Petten) was used, and the spectra were recorded at 4.2 K.

Sulfur and iodine analyses were performed by EPXMA on an electron microscope (JEOL JXA Superprobe 733) operating at 30 kV and using a Tracor TN 2000 detection system. The atomic ratio iodine/sulfur was determined from the intensities in the X-ray spectrum of the K lines of S and I at 2.3 and 29 keV, respectively. Diffusion profiles of iodine into the interior of the doped PTV films were obtained from cuttings of the films embedded in epoxy resin. The cuttings were scanned in the electron microscope, equipped for X-ray energy dispersive spectrometry, monitoring the characteristic X-ray line of iodine (29 keV).

RESULTS AND DISCUSSION

Film quality

In order to obtain fully conjugated PTV, the methoxy precursor solutions must be treated with concentrated hydrochloric acid[10]. Then, elimination starts even without heating, as is evidenced by the evolution of the u.v./vis. spectrum of an HCl-treated methoxy precursor solution (*Figure 1*). The pristine methoxy precursor absorbs at $\lambda = 245$ nm. After addition of HCl a new band arises at $\lambda = 520$ nm within 5 min. Since PTV synthesized via Wittig condensation is known[11] to absorb at $\lambda = 520$ nm, we interpret the new absorption band to indicate the growth of randomly distributed, short PTV segments.

The temperature-dependent evolution of the i.r. spectrum of methoxy precursor films from an HCl-treated chloroform solution is shown in *Figure 2*. The spectrum taken at 30°C shows again that the elimination has started without heating. This follows from the strong absorption band at 930 cm^{-1} caused by the *trans*-vinylene C–H bending. Increasing temperatures give rise to increasing *trans*-vinylene absorptions at 1285 cm^{-1} ($C(sp^2)$–H bending), 1590 cm^{-1} (C=C stretch) and 3015 cm^{-1} (C–H stretch). Quasi-constant intensities are observed for bands at 800 and 1040 cm^{-1}, due to C–H bendings in the thiophene rings. Furthermore, one notes in the 30°C spectrum a band at 1550 cm^{-1}, which disappears upon heating and is assigned to the in-plane O–H bending arising from the protonation of the

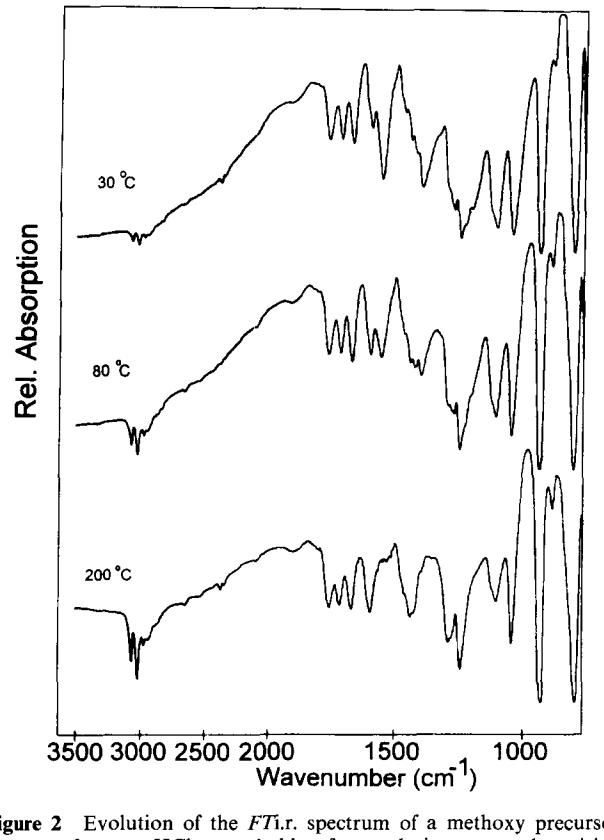

Figure 2 Evolution of the *FT*i.r. spectrum of a methoxy precursor film, cast from an HCl-treated chloroform solution, exposed to rising temperature under vacuum

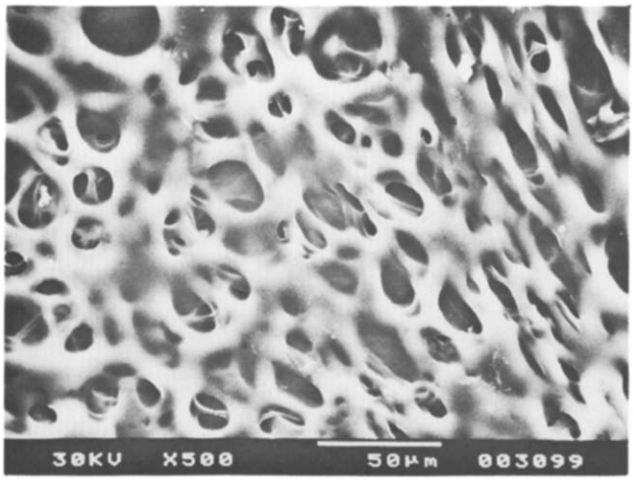

Figure 3 Scanning electron microscopic photograph of an undoped PTV film revealing the porous morphology

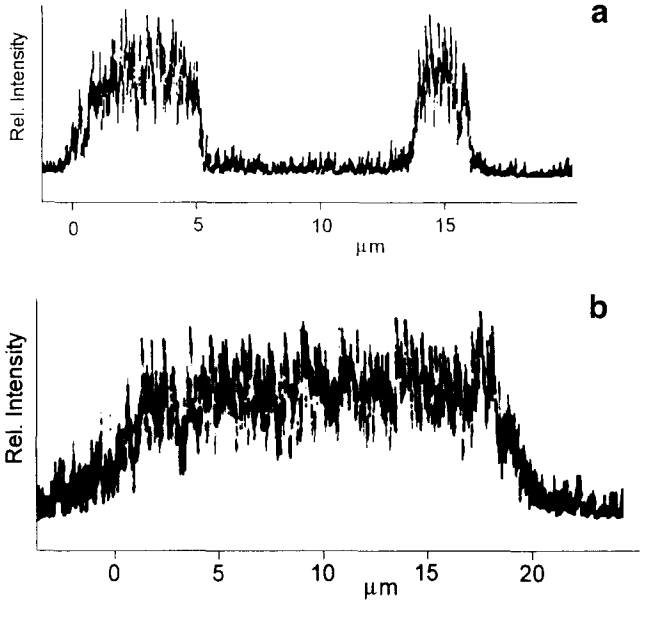

Figure 4 Iodine distribution profiles of (a) a lightly doped PTV film (I/S ratio = 0.073) and (b) a heavily doped film (I/S ratio = 0.40)

methoxy groups of the precursor polymer. The disappearance of this band signals the end of the elimination reaction. Solid state ^{13}C n.m.r. spectra of the PTV films taken at this stage show neither remaining methoxy signals nor signals of carbonyl defects, thus proving the efficiency of the elimination procedure.

Doping and doping characteristics

Secondary electron microscopy images of undoped PTV films (*Figure 3*) show a porous structure, which is caused by the vacuum evaporation of residual solvent during the elimination step. After doping, these voids exhibit a higher concentration of iodine, especially at low doping levels, as was observed by electron diffraction spectroscopy of the doped surfaces. The inhomogeneity in doping levels diminishes, however, at higher degrees of doping. To study the iodine distribution in the interior of the doped PTV films, sections of the films were scanned with a high resolution electron beam and the characteristic X-ray line of iodine (29 keV) was monitored. As an example, Figure 4a gives the distribution profile across a lightly doped film (doped for 40 min at an iodine vapour pressure of 133 Pa) and *Figure 4b* the distribution across a heavily doped film (doped for 24 h in a 3.1×10^{-2} M solution of $^{129}I_2$ in pentane). It follows that doping starts in the surface layers and gradually diffuses into the interior, until finally homogeneous doping is accomplished.

The evolution of electrical conductivity with doping time is shown in *Figure* 5 for iodine vapour pressures of 1333 Pa and 133 Pa. At high vapour pressure (curve a) the conductivity rapidly increases, passes through a maximum and decreases at longer doping times as a result of halogenation of the olefinic bonds in the chain. At low vapour pressure (curve b) a slow doping reaction takes place, resulting in a stabilization of the conductivity for longer doping times at high doping levels. On doping with iodine to a saturation level of 47 wt% iodine (I/S ratio = 0.4) the conductivity has increased by many orders of magnitude to about $10\,\Omega^{-1}\,cm^{-1}$ at room temperature.

These and other results, including i.r. data, show that a slow doping process produces homogeneous doping and that at low vapour pressures (concentrations) no addition of iodine to the carbon–carbon double bonds takes place.

Iodine/sulfur atomic ratios obtained by EPXMA of the films used in the further analyses are summarized in *Table 1*. It should be noted that these I/S ratios—which are strictly speaking surface values—under the appropriate doping conditions are representative of the complete film.

Although the analytical data present a good picture of the dopant content of the doped films, it remains necessary to clarify the nature of the various iodine species present. To do so, ^{129}I Mössbauer spectroscopy was used to analyse quantitatively the presence of I^-, I_3^- and I_5^-. A complete account of this work will be published elsewhere[12]. Here, we present in *Table 1* only the relevant results needed to transform an individual I/S ratio into the (molecular) amount of doping species per monomeric unit. The monoiodide anion I^-, which has been detected as a single line in the Mössbauer spectra of extremely lightly doped polyacetylene[13], is completely absent in the analysed PTV samples (film nos. 6–8 in *Table 1*). The triiodide anion I_3^- is found in minor quantities in film 6 only, while the pentaiodide ion I_5^- is found as the

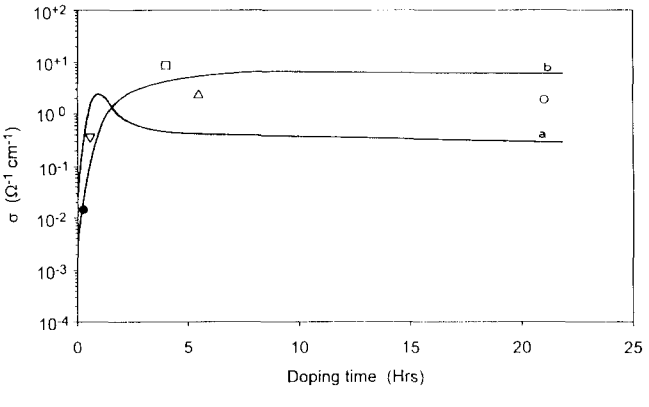

Figure 5 D.c. electrical conductivity of iodine-doped PTV as a function of doping time at a dopant vapour pressure of 1333 Pa (curve a) and 133 Pa (curve b). The room-temperature conductivity of five individual doped films for various doping times at a vapour pressure of 133 Pa are marked. The iodine/sulfur ratio (I/S = y) is: (●) $y = 0.033$; (▽) $y = 0.073$; (□) $y = 0.405$; (△) $y = 0.37$; (○) $y = 0.33$

Table 1 Analytical and doping data of PTV films doped with I_2 in the gas phase (film nos. 1–5) and in $^{129}I_2$ pentane solution (film nos. 6–8), together with variable-range parameters at $T=298$ K for three-dimensional hopping in $[(C_6H_4S)I_y^-]_n$ assuming $\alpha^{-1}=5$ Å (see equation (1))

Film no.	1	2	3	4	5	6	7	8
Dopant time (h)	0.25	0.66	4	5.5	21	72	24	36
Dopant press. (Pa)	133	133	13	133	133			
Dopant conc. (M)						0.00775	0.0155	0.0155
$y=I/S$	0.033	0.073	0.405	0.370	0.330	0.565	0.404	0.470
Dopant species						<5% I_3^- 10–25% I_2 75–90% I_5^-	100% I_5^-	5–15% I_2 85–95% I_5^-
Atomic ratio dopant species/monomer						0.085–0.102	0.081	0.080–0.089
$\sigma(\Omega^{-1}\,cm^{-1})$	0.0144	0.358	8.51	2.25	1.89	1.08	0.704	0.363
$T_0(10^6\,K)$	2.21	1.70	1.30	1.38	1.44	2.86	3.58	3.34
$\nu_0(s^{-1})$	2.5×10^{14}	3.2×10^{15}	2.0×10^{16}	1.1×10^{16}	1.1×10^{16}			
$N(E_F)(10^{20}\,eV^{-1}\,cm^{-3})$	7.6	9.9	16.3	12.2	11.6	5.9	4.7	5.0
ΔE(eV)	0.06	0.05	0.05	0.05	0.05	0.06	0.07	0.07
R(Å)	17	16	14	15	16	19	20	19

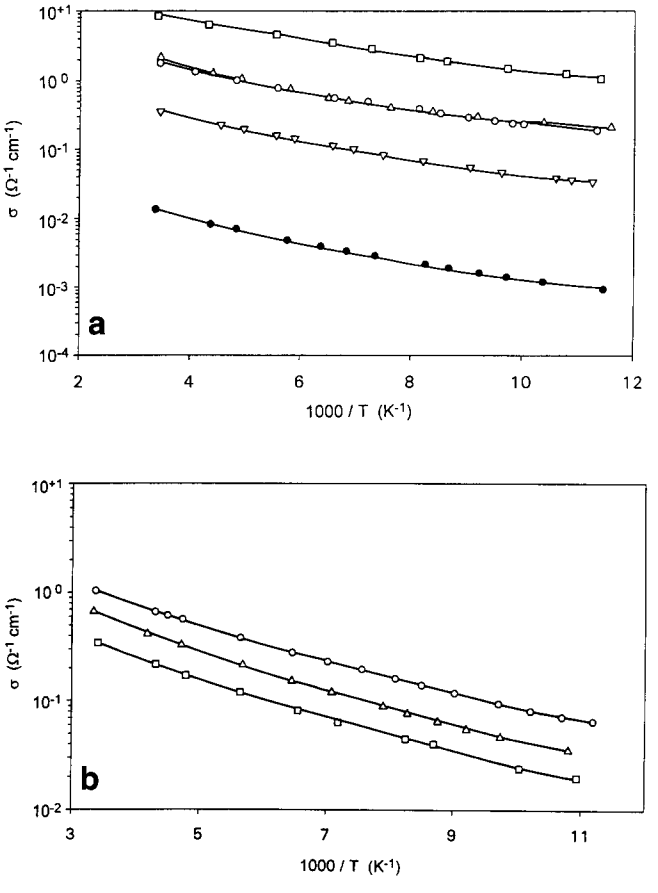

Figure 6 Arrhenius plots of the d.c. conductivity of PTV films doped (a) for 0.25 h (●, no. 1), 0.66 h (▽, no. 2), 4 h (□, no. 3), 5.5 h (△, no. 4) and 21 h (○, no. 5) at an iodine vapour pressure of 133 Pa and (b) for 72 h (○, no. 6) in a 0.00775 M I_2/pentane solution, and 24 h (△, no. 7) and 36 h (□, no. 8) both in 0.0155 M I_2/pentane solution

dominant doping species in films 6–8. Some residual I_2 is observed in films 6 and 8, as a result of adsorption in the interior of these films. It then follows that one I_5^- ion is present per 10–13 monomeric units.

Electrical properties

Valuable information of the applicability of a transport mechanism can be obtained from the temperature dependence of the d.c. electrical conductivity (σ). Such conductivities are measured between 90 and 300 K, and plotted in *Figure 6a* for the gas-phase doped PTV films (nos. 1–5) and in *Figure 6b* for the solution doped films (nos. 6–8) as a function of reciprocal temperature. For all doping levels the conductivity decreases with decreasing temperatures. The lines are continuously curved and hence, the temperature dependence of σ does not obey an Arrhenius law of the form $\sigma=\sigma_0\exp(-E/kT)$. This observation rules out all models involving conduction of electrons in extended states or hopping in band tails. Further examination showed that plots of $\log\sigma$ *versus* $\log T$ are also continuously curved. This rules out Kivelson's[14] intersoliton hopping mechanism, which requires a charged soliton on one chain and a neutral soliton on the next chain. Furthermore, the metal–insulator transition model, expressed by $\sigma(T)=\sigma_0+aT^{1/2}$, as well as a mechanism via conduction along metallic islands, expressed by $\sigma(T)=\sigma_0\exp[-(T_0/T)^{1/2}]$, proved untenable.

An excellent fit was obtained, however, when the d.c. conductivity data were plotted as $\sigma T^{1/2}$ *versus* $T^{-1/4}$ (see *Figure 7*) according to Mott's formula for variable-range hopping in three dimensions[15]:

$$\sigma=\frac{3e^2\nu_0}{128\alpha^2}\left(\frac{T_0}{T}\right)^{1/2}N(E_F)\exp[-(T/T_0)^{-1/4}] \qquad (1)$$

Here, ν_0 represents an attempt frequency, $N(E_F)$ the density of states at the Fermi energy, α the spatial extent of the localized wavefunction, and $T_0=18.1\alpha^3/kN(E_F)$.

Table 1 gives the values of $N(E_F)$, assuming $\alpha^{-1}=5$ Å, and the other parameters evaluated from the data, together with the hopping distance R and the hopping energy ΔE, which were calculated from the expressions derived in Mott's variable-range hopping theory:

$$R=\left(\frac{9}{8\pi\alpha N(E_F)kT}\right)^{1/4} \qquad (2)$$

$$\Delta E=\left(\frac{2\alpha^3k^3T^3}{9\pi N(E_F)}\right)^{1/4} \qquad (3)$$

Although the experimental support for variable-range hopping in iodine-doped PTV is strong, we cannot exclude two alternative conduction mechanisms.

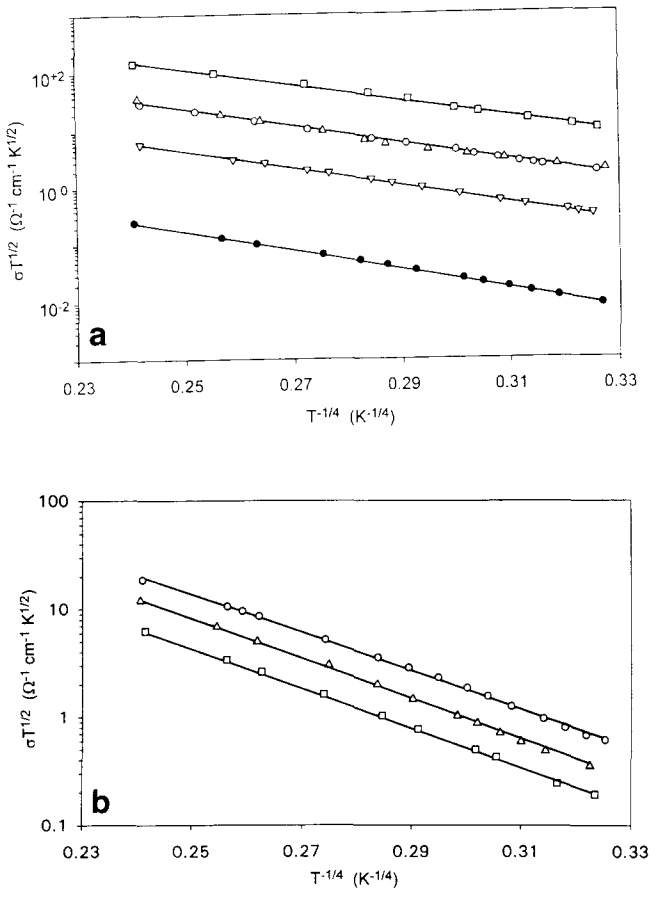

Figure 7 D.c. conductivity data plotted as $\sigma T^{1/2}$ *versus* $T^{-1/4}$, according to the variable-range hopping model: (a) for gas-phase-doped films, (b) for solution-doped films (symbols as in *Figure 6*)

One is the modified hopping model proposed by Schäfer-Siebert and Roth[16], which takes into consideration an extended character of the hopping sites by identifying the localization length as the half conjugation length of the polymer chains. This leads to

$$\sigma T^{1/2} = \sigma_0 T_0^{1/2} \exp[-(T/T_0)^{-1/2}] \quad (4)$$

Using equation (4), we obtained reasonable agreement between calculated σ values and the experimental ones for highly doped films, and we were able to correlate the room-temperature conductivities with T_0. The other model is fluctuation-induced tunnelling between highly conducting regions separated by potential barriers, as proposed by Sheng[17]. This model predicts a temperature dependence of the form:

$$\sigma = \sigma_0 \exp[-T_1/(T + T_0)] \quad (5)$$

The fitting parameters σ_0, T_0 and T_1 are related to the width and height of the potential barriers between the highly conducting regions. Although the fit of the experimental σ values led to unrealistic values for these barrier parameters, we cannot exclude Sheng's model, because the temperature range covered may be too narrow.

CONCLUSIONS

We have shown that PTV films can be homogeneously and reproducibly doped with iodine in pentane solution and in the vapour phase. Mössbauer spectroscopy coupled with electron probe X-ray micro-analysis revealed that the dopant species in highly doped films predominantly exists of I_5^- ions, and corresponds to one dopant species per 10–13 monomer units. Electrical conductivity and number of dopant species depend upon the doping time and the concentration of I_2 (temperature) in the gas phase. Solution as well as gas-phase d.c. electrical conductivity data are consistent with the variable-range hopping mechanism.

ACKNOWLEDGEMENTS

We are grateful to Professor Dr G. Van Tendeloo and Dr X. B. Zhang (University of Antwerpen, RUCA) for the electron microscopic analyses and to Professor Dr G. Langouche and Dr J. Wauters (Catholic University, Leuven) for the Mössbauer measurements. W.H. thanks the Belgian National Science Foundation (NFWO) for a predoctoral grant. This text presents research results of the Belgian Programme on Interuniversity Attraction Poles initiated by the Belgian State (Prime Minister's Office), Science Policy Programming. Scientific responsibility, however, is assumed by the authors.

REFERENCES

1 Jen, K. Y., Jow, R., Eckhardt, H. and Elsenbaumer, R. L. *Polym. Mater. Sci. Eng.* 1987, **56**, 49
2 Kossmehl, G. A. in 'Handbook of Conducting Polymers' (Ed. T. A. Skotheim), Marcel Dekker, Basel, 1986, Ch. 10
3 Kanbe, M. and Okawara, M. *J. Polym. Sci. (A-1)* 1968, **6**, 1058
4 Karasz, F. E., Capistran, J. D., Gagnon, D. R., Lenz, R. W. and Antoun, S. *Polymer* 1987, **28**, 567
5 Murase, I., Ohnishi, T., Noguchi, T. and Hirooka, M. *Polym. Commun.* 1987, **28**, 229
6 Lahti, R. M., Modarelli, D. A., Denton, F. R., Lenz, R. W. and Karasz, F. E. *J. Am. Chem. Soc.* 1988, **110**, 7258
7 Eevers, W., De Schrijver, D., Dierick, T., Peten, C., Van Der Looy, J. and Geise, H. J. *Synth. Met.* 1992, **51**, 329
8 Gibb, T. C. in 'Principles of Mössbauer Spectroscopy', Chapman and Hall, London, 1976
9 Kaindl, G., Wortmann, G., Roth, S. and Menke, K. *Solid State Commun.* 1982, **41**, 75
10 Eevers, W. PhD thesis, University of Antwerpen (UIA), 1993 (in Dutch)
11 Geens, R. PhD thesis, University of Antwerpen (UIA), 1988 (in Dutch)
12 Eevers, W., De Wit, M., Briers, J., Geise, H. J., Langouche, G., Wauters, J. and Claeys, M. to be published
13 Matsuyama, T., Sakai, H., Yamaoka, H., Maedea, Y. and Shirakawa, H. *J. Phys. Soc. Japan* 1983, **52**, 2238
14 Kivelson, S. *Phys. Rev. Lett.* 1981, **46**, 1344
15 Mott, N. F. *Phil. Mag.* 1969, **19**, 835
16 Schäfer-Siebert, D. and Roth, S. *Synth. Met.* 1989, **28**, D369
17 Sheng, P. *Phys. Rev. (B)* 1980, **21**, 2180